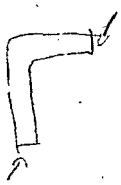

Connections for Welded Continuous Portal Frames

Progress Report No. 4: Part II—"Theoretical Analysis of Straight Knees"*

Theoretical analysis for straight knees of a rigid frame structure forming the basis for comparing experimental results with theory. Stresses rotations and deflections are considered

by Lynn S. Beedle, A. A. Topractsoglou and Bruce G. Johnston

Foreword

Part I of this report appeared in the July 1951 issue of *Welding Research Supplement*. It included a presentation of test results for 15 welded corner connections of various types and a discussion of knee requirements.

Part II, presented here, contains the theoretical analysis for straight knees, forming the basis for a comparison of experimental results with theory. Stresses, rotations and deflections are considered.

Part III of this Progress Report No. 4 will appear in a later issue of THE WELDING JOURNAL and will include the discussion of test results and the conclusions.

I. ELASTIC ANALYSIS

FBLEICH[25†] has proposed approximate methods for stress analysis and design of square knees. He assumes that for square knees: "... where the ratio of the length of the restraining arm to its depth is equal to or larger than one, the Navier theory yields sufficiently accurate results and one may determine the fiber stresses and shear stresses according to the conventional theory." By "restraining arm" is meant the arm AD, which acts to restrain the girder, Fig. 58.†

In the rolled section adjacent to the knee (at section AD) it has also been assumed that the ordinary beam theory applies for predicting stresses and deformations.

1. Stress Analysis of Straight Knees Without Diagonal Stiffeners*

(a) Identical Rolled Shapes

Consider connection type 7, shown in Fig. 59 (*a*). The stresses in the knee $ABCD$ are found by making the following assumptions:

1. The bending moment at the section AD is carried entirely by the flanges. In the knee shown, $M_r = V(L - (d/2))$ and the portion of the flange force, F, due to bending is given by

$$F = \frac{M_r}{d} = V\left(\frac{L}{d} - \frac{1}{2}\right)$$

The designation M_r will be used throughout this report to indicate the moment at the end of the rolled section and beginning of the knee, whether it be straight, curved or haunched. M_h is then used to denote the "haunch" moment or moment at the intersection of the neutral lines of the girder and column. In the above expression the remaining terms are defined by Fig. 59.

2. Shearing force, V, is taken by the web and is uniformly distributed.

3. The normal force, N, is considered. It is assumed to act at the flanges, however, as shown in Fig. 60.

4. The flange force varies linearly between D and C, with maximum at D and zero at C.

5. Stress concentrations are not considered.

6. Restraint due to bending of individual flange elements is neglected.

Fig. 59 (*c*) shows the forces acting on the knee. Taking into account the above assumptions, the forces and stresses are applied to the flange element as shown in Fig. 61 (*a*). Stresses on the web are indicated in Fig. 61 (*b*). Subscripts *o* and *i* represent "outside" and "inside" forces or stresses, respectively. Neglecting the

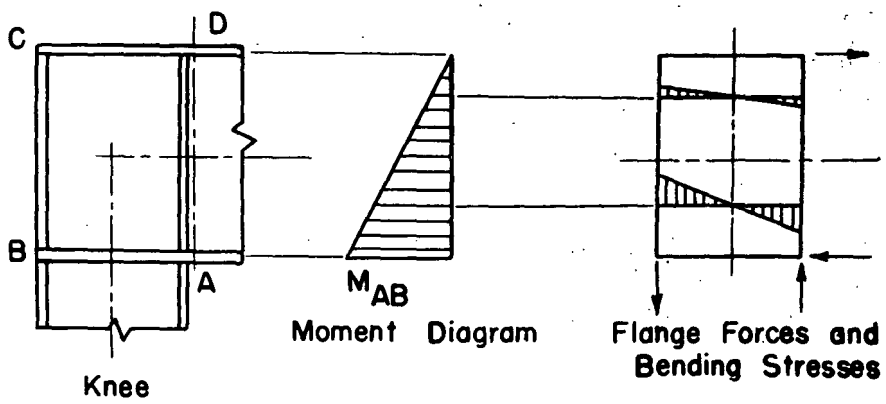

Fig. 58 Assumed moment, forces and stresses on typical straight knee

---

Lynn S. Beedle is Assistant to the Director, Fritz Engineering Laboratory. **A. A. Topractsoglou** is Assistant Professor of Civil Engineering with the University of Texas; formerly, Instructor at Lehigh University. **Bruce G. Johnston** was formerly Director of Fritz Engineering Laboratory, now Professor of Structural Engineering at the University of Michigan.

* This work has been carried out as a part of an investigation sponsored jointly by the Welding Research Council and the Department of the Navy with funds furnished by the following: American Institute of Steel Construction, American Iron and Steel Institute, Column Research Council (Advisory), Institute of Research, Lehigh University, Office of Naval Research (Contract No. 39303), Bureau of Ships and Bureau of Yards and Docks.

† Superior numbers indicate reference numbers listed in Part I.

* The terms "square" and "straight" are both used to designate a connection in which the girder and column rolled sections are joined at right angles without the use of additional haunch or bracket material.

† Figure numbers continue the same sequence commenced in Part I.

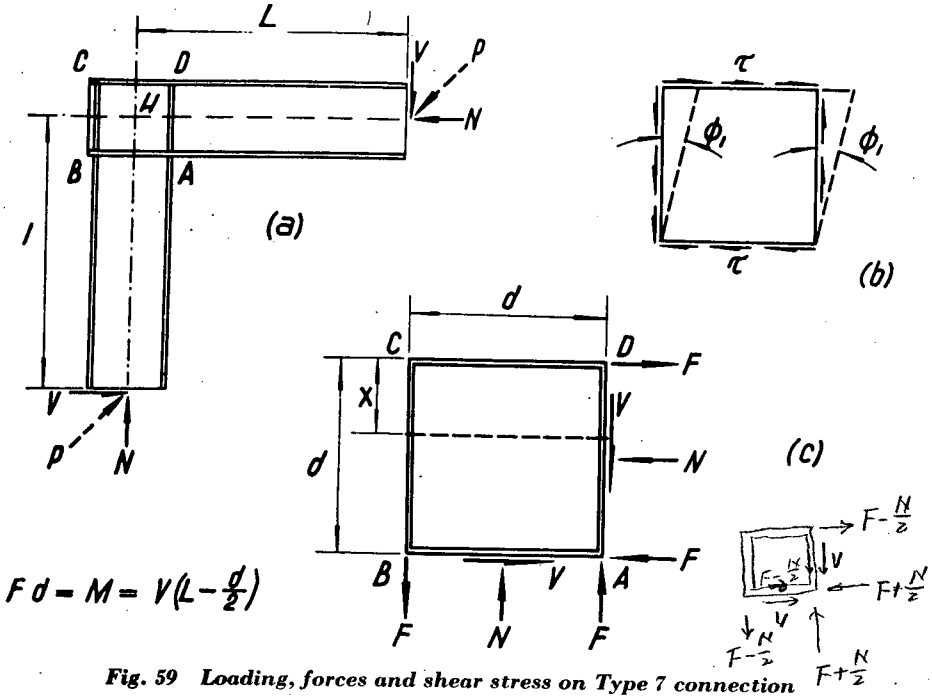

Fig. 59 Loading, forces and shear stress on Type 7 connection

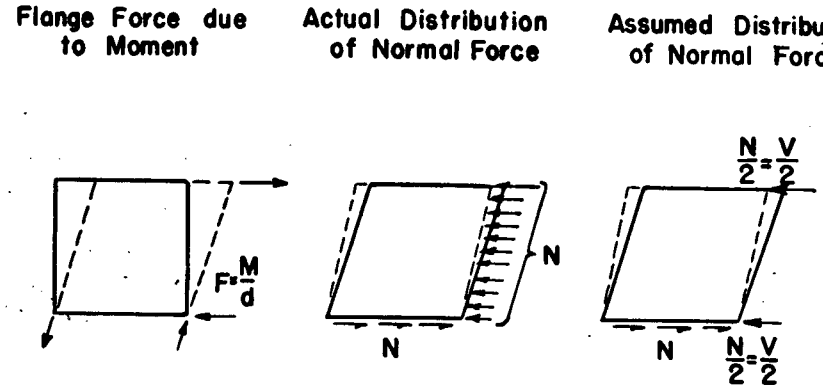

Fig. 60 Distribution of normal force

web and noting that $N = V$, the outside flange force is given by

$$F_o = \frac{M_r}{d} - \frac{N}{2}$$

$$F_o = \frac{V(L - d/2)}{d} - \frac{V}{2}$$

$$F_o = V\left(\frac{L}{d} - 1\right)$$

At the inside flange,

$$F_i = \frac{M_r}{d} + \frac{V}{2} = \frac{V(L - d/2)}{d} + \frac{V}{2}$$

$$F_i = \frac{VL}{d}$$

Computing the shear stresses τ on the web panel,

$$\tau_o = \frac{F_o}{A_w} = \frac{V}{A_w}\left(\frac{L}{d} - 1\right)$$

where A_w = area of the web; and

$$\tau_i = \frac{F_i - V}{A_w} = \frac{V(L/d) - V}{A_w}$$

$$\tau_i = \frac{V}{A_w}\left(\frac{L}{d} - 1\right) \qquad (1)$$

Thus

$$\tau_o = \tau_i$$

The stress distributions in the various elements are as follows:

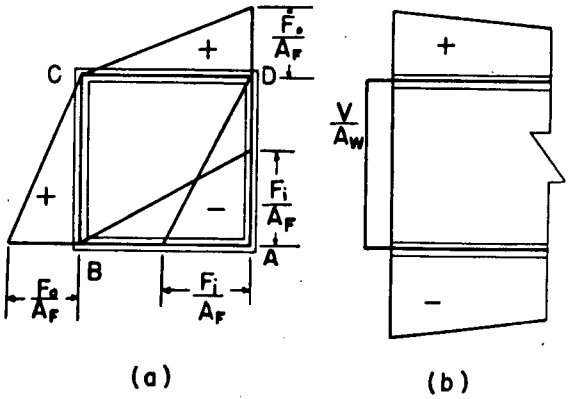

Fig. 62 Assumed stress distribution in flanges and web

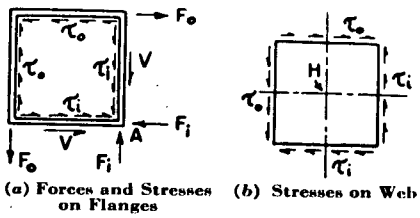

Fig. 61 Loading on flanges and on web

1. The knee web is loaded in pure shear (Fig. 61 (*b*).)

2. The stresses in the flanges forming the knee are distributed as shown in Fig. 62 (*a*), where the ordinate represents the mean normal stress in the flange cross section. Tensile stresses are plotted external to the knee.

3. To the right of section AD, the stresses are given by Fig. 62 (*b*).

The stress distributions shown in Fig. 63 correspond to those of Fig. 62 (*b*) except that they are computed on the basis of ordinary beam theory. Comparing the resulting stresses at section AD for a connection with 14WF30 members indicates a difference of about 8% which will be neglected.

The theoretical stresses may be compared to experimentally determined values on the basis of either load or moment. The latter will be used hereafter.

From the point of view of balanced de-

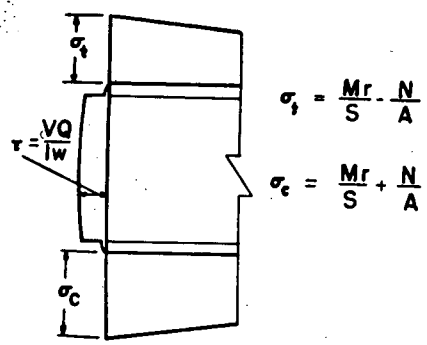

Fig. 63 Distribution of stress in girder flanges and shear stress distribution at section AD according to conventional beam theory

sign the shear stress at point H of Fig. 61 should reach the yield value at the same external bending moment at which point A reaches the yield point in combined bending and direct stress. (Actual combined stresses will be higher elsewhere, but for engineering purposes it is considered that examination of the separate stresses at these two points is adequate.)

The stress patterns at other places in the connections were measured and a later paper will present the results as compared with the theoretically predicted values.

It is of importance that yielding due to shear force does not occur in unstiffened knee webs below the flexural yield load. Such yielding may cause large deformations. Conventional design neglects the possibility of such shear deformation and it is not practical to attempt to take it into account in routine deformation computations. Therefore, the investigation of yielding in an unstiffened knee web is desirable.

Given the square knee loaded as described previously, the problem is to find the moment under which yielding due to shear force occurs in the web.

According to the assumptions used herein, shear stresses in the knee web are uniform along horizontal sections. The actual bending stresses at section DA cause maximum shearing stresses to occur near the center of the knee web, decreasing toward the flanges. This maximum value is somewhat greater than the average uniform value, but this increase is neglected for the time being.

The following values will be substituted into Equation 1:

$$A_w = (d)(w)$$

and

$$V = \frac{M_h}{L}$$

Thus

$$\tau = \frac{M_h}{wd^2}\left(1 - \frac{d}{L}\right) \qquad (2)$$

Since the normal stresses are negligible at the center of the knee, a state of pure shear may be assumed, and

$$\sigma_1 = -\sigma_2 = \tau$$

Thus the web yields when the maximum shear stress equals

$$\tau_y = \frac{\sigma_y}{2}^*$$

in which σ_y = lower yield-point stress of web material as determined in a simple tension test. Thus from Equation 2, substituting for τ the value $\sigma_y/2$,

$$M_{h(\tau)} = \frac{\sigma_y wd^2}{2(1 - d/L)} \qquad (3)$$

where $M_{h(\tau)}$ is the moment at which yielding occurs due to shear force in the web (point H, Fig. 61 (b)).

* The maximum shear stress theory is conservative. More accurately, by the octahedral shear stress theory, $\tau_y = 0.578\sigma_y$.

Table 1—Comparison of Yield Strengths Due to Shear and Due to Flexure for Various Rolled Shapes

Section (1)	S (2)	w (3)	d (4)	A (5)	$\frac{M_{h(\tau)}}{M_{h(\sigma)}}$ (L/d = 6.0) (6)	$\frac{M_{h(\tau)}}{M_{h(\sigma)}}$ ($L = L_u$) (7)
14WF30	41.80	0.270	13.90	8.81	0.726	0.693
8B13	9.88	0.230	8.00	3.83	0.867	0.822
21WF82	168.00	0.499	20.86	24.10	0.754	...
6B12	7.24	0.230	6.00	3.53	0.666	...
24WF110	274.40	0.510	24.16	32.36	0.633	...
8WF31	27.40	0.288	8.00	9.12	0.395	0.364

The stress at point A, Fig. 61 (a), is given by

$$\sigma_c = \frac{M_r}{S} + \frac{N}{A} = \frac{M_r}{S} + \frac{V}{A}$$

Since

$$M_h = VL$$

and

$$M_r = M_h(1 - (d/2L))$$

then

$$\sigma_c = M_h\left[\frac{1 - (d/2L)}{S} + \frac{1}{AL}\right]$$

$$M_{h(\sigma)} = \left[\frac{\sigma_y}{\left(\frac{1 - (d/2L)}{S}\right) + \frac{1}{AL}}\right] \qquad (4)$$

in which $M_{h(\sigma)}$ is the moment at the haunch when yielding occurs due to flexure and direct stress at the critical section DA.

If the ratio $M_{h(\tau)}/M_{h(\sigma)}$ is formed, it will be possible to determine whether a connection fabricated of a particular rolled shape will yield in the web (shear) or in the rolled shape (flexure). So long as the ratio is greater than 1.0, yielding due to shear force within the knee should not occur.

Then from Equations 3 and 4

$$\frac{M_{h(\tau)}}{M_{h(\sigma)}} = \frac{\frac{\sigma_y wd^2}{2(1 - d/L)}}{\sigma_y}\left[\frac{1 - \frac{d}{2L}}{S} + \frac{1}{AL}\right]$$

$$\frac{M_{h(\tau)}}{M_{h(\sigma)}} = \frac{wd^2}{2\left(1 - \frac{d}{L}\right)}\left[\frac{1 - \frac{d}{2L}}{S} + \frac{1}{AL}\right] \qquad (5)$$

Some commonly available rolled sections have been investigated using Equation 5 and the results are given in Table 1.

The calculation shows that "shear yielding" will usually occur prior to yielding in flexure (based on a constant L/d ratio of 6.0). An alternate basis for comparison would be obtained if the value "L_u" were selected such that Ld/bt = 600. . .a limiting case for lateral buckling. Three examples were selected and the resulting ratio is shown in Column 7. The same general trend is observed, the ratio being particularly low for the 8WF31 "column" section.

(b) Stress Analysis: Dissimilar Rolled Shapes ($d_1 \neq d_2$)

Reference is made to Fig. 64 and the assumptions stated earlier. It will be further assumed that $d_2 < d_1$. The subscripts 1 and 2 refer to members 1 and 2. Then

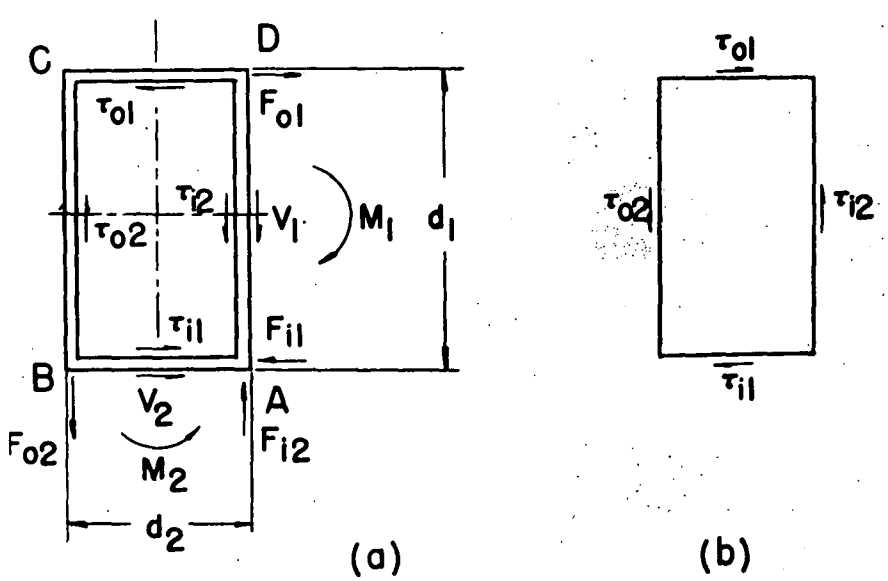

Fig. 64 Knee joining dissimilar rolled shapes; indicated are forces and shear stresses

$$F_{o1} = \frac{M_{r1}}{d_1} - \frac{V}{2}$$

$$M_{r1} = V\left(L - \frac{d_2}{2}\right)$$

$$F_{o1} = \frac{V}{d_1}\left[L - \frac{(d_1 + d_2)}{2}\right] \quad (6)$$

Also

$$F_{i1} = \frac{M_{r1}}{d_1} + \frac{V}{2}$$

$$F_{i1} = \frac{V}{d_1}\left[L + \frac{(d_1 - d_2)}{2}\right] \quad (7)$$

Similarly,

$$\left.\begin{aligned} F_{o2} &= \frac{V}{d_2}\left[L - \frac{(d_1 + d_2)}{2}\right] \\ F_{i2} &= \frac{V}{d_2}\left[L + \frac{(d_2 - d_1)}{2}\right] \end{aligned}\right\} \quad (8)$$

Since

$$\tau = \frac{F}{A_w}$$

$$\tau_{o1} = \frac{F_{o1}}{wd_2} = \frac{V}{wd_1d_2}\left[L - \frac{(d_1 + d_2)}{2}\right]$$

$$\tau_{i1} = \frac{F_{i1} - V}{wd_2} = \frac{V}{wd_1d_2}\left[L + \frac{(d_1 - d_2)}{2}\right] = \frac{V}{wd_2} = \frac{V}{wd_1d_2}\left[L - \frac{(d_1 + d_2)}{2}\right]$$

$$\tau_{o2} = \frac{F_{o2}}{wd_1} = \frac{V}{wd_1d_2}\left[L - \frac{(d_1 + d_2)}{2}\right]$$

$$\tau_{i2} = \frac{F_{i2} - V}{wd_1} = \frac{V}{wd_1d_2}\left[L + \frac{(d_2 - d_1)}{2}\right] - \frac{V}{wd_1} = \frac{V}{wd_1d_2}\left[L - \frac{(d_1 + d_2)}{2}\right]$$

All the τ's are equal and the web, neglecting small bending effects, is in a state of pure shear,

$$\tau = \frac{V}{wd_1d_2}\left[L - \frac{(d_1 + d_2)}{2}\right] \quad (9)$$

Then

$$\tau = \frac{M_h}{wd_1d_2}\left[1 - \frac{(d_1 + d_2)}{2L}\right] \quad (10)$$

An examination of initial yield in the web due to shear force and in the flange due to bending, now follows. Member "2" is smaller than member "1" and flexural yield will occur first at point A on section AB in Fig. 64. Yielding due to shear force occurs when

$$\tau = \frac{\sigma_y}{2}$$

Therefore, from Equation 10,

$$M_{h(\tau)} = \frac{wd_1d_2\sigma_y}{2}\left[\frac{1}{1 - \dfrac{d_1 + d_2}{2L}}\right]^* \quad (11)$$

At point A, from Equation 4,

$$\sigma_y = \frac{M_{r2}}{S_2} + \frac{V}{A_2} = \frac{M_{2r}}{S_2} + \frac{M_h}{A_2L}$$

$$\sigma_y = M_h\left[\frac{1 - d_1/2L}{S_2} + \frac{1}{A_2L}\right]$$

$$M_{h(\sigma)} = \frac{\sigma_y}{\dfrac{(1 - d/2L)}{S_2} + \dfrac{1}{A_2L}} \quad (12)$$

Applying Expressions 11 and 12 to connection test P (Type 7 knee using 8WF31 and 14WF30 shapes) and using the dimensions and properties determined from the specimens,

$$M_{h(\tau)} = 724 \text{ in.-kips.}$$
$$M_{h(\sigma)} = 1140 \text{ in.-kips.}$$

(The magnitude of $M_{h(\tau)}$ is plotted as a horizontal line in Fig. 19, Part I.)

The ratio of the two moments is

$$\frac{M_{h(\tau)}}{M_{h(\sigma)}} = \frac{724}{1140} = 0.619$$

Comparing this result with the calculations of Table 1, it is evident that the worst case is that in which the two section depths are not equal (compare 0.726 with 0.619).

Earlier in this report it was assumed that the shear stress was uniformly distributed across the web. However, according to F. Bleich's original assumption, shear stresses would be distributed in parabolic form. Thus,

$$\tau_{max.} = \frac{V_kQ_k}{I_kw_k} \quad (13)$$

where the subscripts, k, denote dimensions in the knee, Q_k is the static moment of one-half the cross section and w_k is the web thickness. Since, from Fig. 64

$$V_k = F_{o1}$$

then from equations 6, 9 and 13

$$\frac{\tau_{max.}}{\tau_{av.}} = \frac{Q_kd_2}{I_k} \quad (14)$$

Using the dimensions for test connection P,

$$\frac{\tau_{max.}}{\tau_{av.}} = 1.15$$

or the maximum shear at point H is 15% greater than the average value computed according to Equation 9. The more accurate predicted value for $M_{h(\tau)}$ is then,

$$M_{h(\tau)} = \frac{724}{1.15} = 630 \text{ in.-kips.}$$

Better agreement with the experimentally-determined value is obtained as is evident from Fig. 19, Part I. The previous expressions for "shear" yielding could all be modified by an appropriate factor Q_kd_k/I_k. However, since this would have the effect of decreasing the ratio $M_{h(\tau)}/M_{h(\sigma)}$ in Table 1, which values are already less than unity, the modification only lends further emphasis to the necessity for additional stiffening to prevent undesirable shear deformation.

The analysis presented above can at best only be considered as approximate. First of all the boundary conditions are not exactly as assumed. When the flanges are thick in proportion to the depth of the section they provide additional restraint which will enable the knee to carry more load before yielding due to shear force commences.

Secondly, residual stress is built up in the knee due to welding of the stiffeners. Presumably this alone would cause yielding to occur at a lower load than predicted.

2. *Rotation Analysis*

The knee rotation is made up of two parts: (1) Rotation due to shear, designated as γ, and (2) rotation due to bending designated as β. Since a comparison is to be made later with experimentally-determined values there is a third component to be considered: (3) Rotation due to bending of the rolled section over the length, r, between the knee and point of rotation measurement, designated as ϕ_r.

Therefore, the total knee rotation is

$$\theta = \gamma + \beta + \phi_r \quad (15)$$

(a) Type 7 Connection with Identical Members* ($d_1 = d_2$)

The assumptions of the first section will be used. From Fig. 59 (*b*) and Equation 2, the rotation due to shear is,

$$\gamma_7 = \tau/G$$

$$\gamma_7 = \frac{M_h}{wd^2G}\left(1 - \frac{d}{L}\right) \quad (16)$$

where

γ_7 = shear rotation of Type 7 connection.
G = modulus of elasticity in shear.

The rotation due to bending moment may be determined from the elongations or contractions of the flanges. As stated earlier, it is assumed that the web carries all the shear force and the flange elements carry the direct stresses.

The flange stresses were shown in Fig. 62 (*a*). Depending on the boundary conditions assumed, the flanges will deform into one of the patterns shown in Fig. 65.

In Fig. 65 (*a*), the tension flanges BC and CD elongate, but the shortening of the compression flange is not considered. In this case $\beta = 2\theta_a$. In Fig. 65 (*b*), the extension and shortening of all four flanges is considered according to the assumed stress distribution of Fig. 62; then $\beta = 2\theta_b$. In both Figs. 65 (*a*) and (*b*) point A does not shift with respect to point C since the rotation resulting from such motion is included in the shear deformation determined from Equation 16.

Since all of the extensions and contractions are small quantities, the angle θ_a will very nearly equal θ_b. It will be assumed so; because of its simplicity, the deformation pattern of Fig. 65 (*a*) will also be assumed throughout this report.

Let δ be the extension of the tension flanges BC and CD due to the average flange stress $\sigma_t/2$. Then

$$\delta = \frac{\sigma_t d}{2E}$$

and

* It is evident from this expression that the member with the thickest web should be made continuous into the knee so that the greater thickness of web will assist in carrying the shear force.

* Designation of connection types was established in Part I, Fig. 4; straight connections included in the test program are shown in Fig. 8.

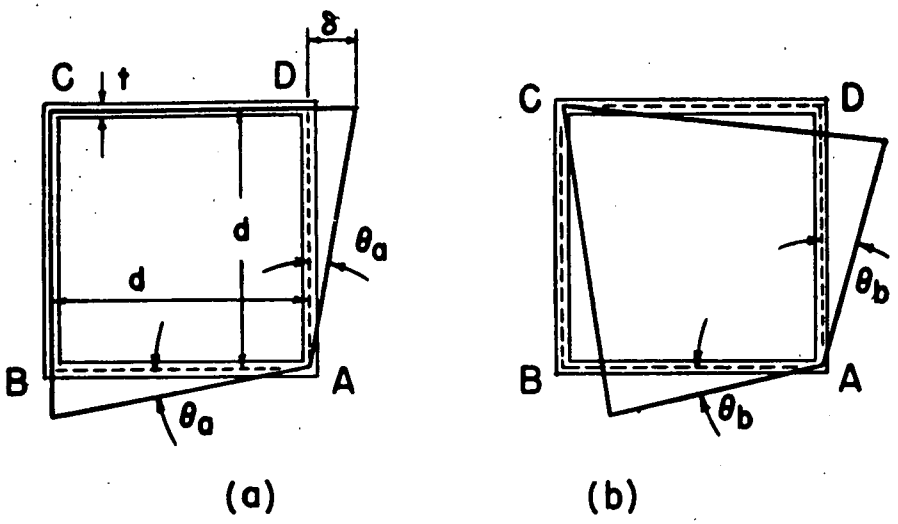

Fig. 65 Assumed knee deformations for members of equal depth

$$\theta_a = \frac{\delta}{d} = \frac{\sigma_t}{2E}$$

The total bending rotation at the knee is

$$\beta = 2\theta_a = \frac{\sigma_t}{E}$$

Neglecting the influence of direct stress,

$$\sigma_t = \frac{(M_r)(c)}{I_F} = \frac{M_h\left(1 - \frac{d}{2L}\right)\left(\frac{d}{2}\right)}{I_F}$$

Then

$$\beta_7 = \frac{M_h\left(1 - \frac{d}{2L}\right)(d)}{2EI_F} \qquad (17)$$

where

$$I_F = 2A_F\left(\frac{d}{2} - \frac{t}{2}\right)^2$$

A_F = flange area.
t = flange thickness.

The rotation, ϕ_r, due to flexure of the rolled section over lengths r is given by

$$\phi_r = 2r\left(\frac{M_r}{EI}\right)$$

$$\phi_r = 2r\frac{M_h}{EI}\left(1 - \frac{d}{2L}\right) \qquad (18)$$

Then the total rotation from Equation 15 is given by a summation of the values determined from equations 16, 17 and 18, or

$$\theta_7 = (\gamma_7 + \beta_7 + \phi_r)$$

$$\theta_7 = \left[\frac{M_h}{wd^2G}\left(1 - \frac{d}{L}\right) + \frac{M_h}{2EI_F} \times \left(1 - \frac{d}{2L}\right)d + \frac{M_h\left(1 - \frac{d}{2L}\right)}{EI} \cdot 2r\right]$$

$$\theta_7 = M_h\left[\frac{\left(1 - \frac{d}{L}\right)}{wd^2G} + \frac{\left(1 - \frac{d}{2L}\right)d}{2EI_F} + \frac{\left(1 - \frac{d}{2L}\right)2r}{EI}\right] \qquad (19)$$

Since the test program did not include a Type 7 connection with identical members the calculation will not be carried further.

(b) Type 7 Connection with Dissimilar Members ($d_1 \neq d_2$)

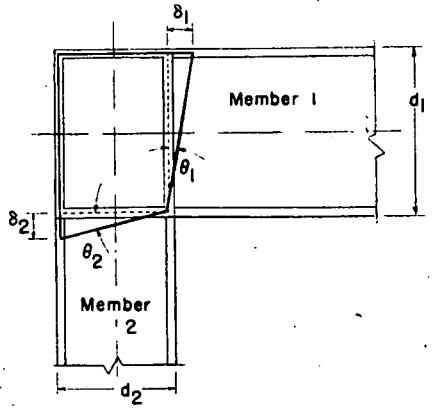

Fig. 66 Assumed knee deformations for members of unequal depth

From Equation 10,

$$\gamma_7 = \frac{\tau}{G} = \frac{M_h}{wd_1d_2G}\left[1 - \frac{(d_1 + d_2)^2}{2L}\right] \qquad (20)$$

Fig. 66 shows the flange deformations (corresponding with Fig. 65) which are the basis for computing the bending rotations. From Fig. 66

$$\beta_7 = \theta_1 + \theta_2$$

$$\theta_1 = \frac{\delta_1}{d_1} = \frac{\sigma_{t1}d_2}{2Ed_1}$$

$$\theta_2 = \frac{\delta_2}{d_2} = \frac{\sigma_{t2}d_1}{2Ed_2}$$

Since

$$\sigma_{t1} = \frac{M_h\left(1 - \frac{d_2}{2L}\right)d_1}{2I_{F1}}$$

and

$$\sigma_{t2} = \frac{M_h\left(1 - \frac{d_1}{2L}\right)d_2}{2I_{F2}}$$

then

$$\beta_7 = \frac{1}{2E}\left[\frac{d_2\sigma_{t1}}{d_1} + \frac{d_1\sigma_{t2}}{d_2}\right]$$

$$\beta_7 = \frac{M_h}{4E}\left[\frac{\left(1 - \frac{d_2}{2L}\right)d_2}{I_{F1}} + \frac{\left(1 - \frac{d_1}{2L}\right)d_1}{I_{F2}}\right] \qquad (21)$$

The rolled section rotations are computed from

$$\phi_{r1} = r_1\left[\frac{M_h}{EI_1}\left(1 - \frac{d_2}{2L}\right)\right]$$

$$\phi_{r2} = r_2\left[\frac{M_h}{EI_2}\left(1 - \frac{d_1}{2L}\right)\right]$$

Assuming the r-distances and E-values identical for the two members,

$$\phi_r = \phi_{r1} + \phi_{r2}$$

$$\phi_r = r_1\frac{M_h}{E}\left[\frac{\left(1 - \frac{d_2}{2L}\right)}{I_1} + \frac{\left(1 - \frac{d_1}{2L}\right)}{I_2}\right] \qquad (22)$$

Combining Equations 20, 21 and 22, the total rotation of a Type 7 connection with dissimilar members is given by

$$\theta_7 = (\gamma_7 + \beta_7 + \phi_r)$$

$$\theta_7 = M_h\left[\frac{1 - \frac{(d_1 + d_2)}{2L}}{wd_1d_2G} + \frac{1}{4E}\left\{\frac{\left(1 - \frac{d_2}{2L}\right)d_2}{I_{F1}} + \frac{\left(1 - \frac{d_1}{2L}\right)d_1}{I_{F2}}\right\} + \frac{r}{E}\left\{\frac{\left(1 - \frac{d_2}{2L}\right)}{I_1} + \frac{\left(1 - \frac{d_1}{2L}\right)}{I_2}\right\}\right] \qquad (23)$$

Computing the total rotation for connection P,

$$\theta_7 = (\gamma_7 + \beta_7 + \phi_r)$$

$$\theta_7 = (2.440 + 1.171 + 0.777) \times 10^{-6} M_h \text{ rad.}$$

$$\theta_7 = 4.39 \times 10^{-6} M_h \text{ rad.}$$

This theoretical moment-angle change relationship is plotted with the experimental values in Fig. 19, Part I. The relative magnitude of the components γ_7, β_7 and ϕ_r may be seen in the calculation above and it will be noted that the shear component is the largest.

(c) Connections with Diagonal Stiffeners

1. Type 2 Connections. Rotations due to shear in the square knee $ABCD$ reinforced with diagonal stiffeners (Fig. 67) will be found by making the following assumptions:

(*a*) The thrust of the two compressive forces V_aL/d is taken by the stiffeners at point A. The necessity for the designation, V_a, will be described later.

(*b*) The stress in the diagonal stiffener varies linearly from a maximum at A to zero at C. It was assumed earlier that the force, F_o, was transmitted uniformly to the web along the length CD (Fig. 67). A portion of this shear, then, is transmitted to the stiffener in proportion to the length of web intercepted by it.

(*c*) Stress concentrations are disregarded.

From assumption (*b*) it follows that the stiffener stresses cause uniform shear, τ_s, in the web of the knee. See Fig. 67 (*b*).

The moment required to deform a Type 2 connection in shear consists of two parts: (*a*) The moment necessary to shorten the

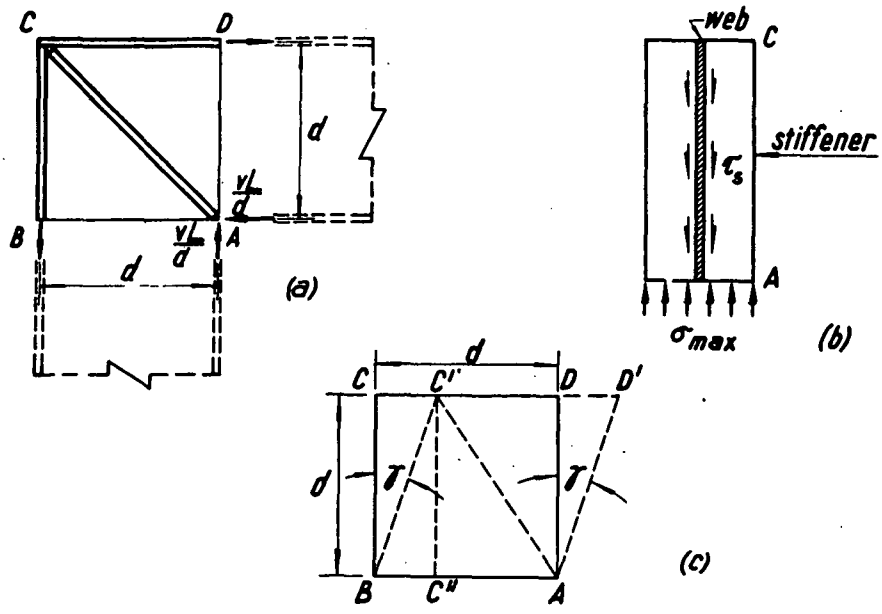

Fig. 67 Loading, forces and deformation in Type 2 connection

diagonal stiffener, and (*b*) that required to deform the web. Thus the presence of a diagonal reduces the shear stress in the web but a portion of the flange force is transmitted by the web without assistance from the diagonal stiffener.

The total contraction in the diagonal stiffener, ΔL_1, is determined from

$$\epsilon = \frac{\sigma}{E} = \frac{\Delta L_1}{\sqrt{2}d}$$

and

$$\Delta L_1 = \frac{\sigma_A}{\sqrt{2}}\frac{d}{E}$$

where

σ_A = stress at point A, Fig. 67.

$$\sigma_A = \frac{\sqrt{2}F_{ia}}{A_s} = \frac{\sqrt{2}V_a L}{A_s d} = \frac{\sqrt{2}M_{ha}}{A_s d}.$$

A_s = area of diagonal stiffener.

and the subscripts a relate to the moment associated with contraction of the stiffener. Then

$$\Delta L_1 = \frac{M_{ha}}{A_s E} \qquad (24)$$

Consider the action of the web with the stiffener removed. Due to shearing forces this web will take the shape $ABC'D'$, Fig. 67 (*c*). The following relations are then obtained:

$$C'C'' = d$$
$$BC'' = d \sin \gamma_2 \cong d\gamma_2$$
$$C''A = d(1 - \gamma_2)$$

where γ_2 = the shearing strain in Type 2 connections. The change in length ΔL_2 along the diagonal line AC is given by

$$\Delta L_2 = CA - C'A = d\sqrt{2} - \sqrt{d^2 + d^2(1 - \gamma_2)^2}$$

The second term may be expanded as a series, and neglecting terms of higher degree,

$$\Delta L_2 = \frac{\gamma_2 d}{\sqrt{2}} \qquad (25)$$

Since this change in length must be equal to the contraction in the stiffener, then

$$\Delta L_1 = \Delta L_2$$

and from equations 24 and 25,

$$\frac{M_{ha}}{A_s E} = \frac{\gamma_2 d}{\sqrt{2}}$$

$$M_{ha} = \frac{\gamma_2 A_s E d}{\sqrt{2}} \qquad (26)$$

In considering the second of the two moments mentioned above, it will be remembered that Equation 2 was developed for a square knee with vertical stiffener extensions of the inner beam and column flanges as sketched in Fig. 59. Such vertical stiffeners are not present in Type 2 connections. However, the web material will act somewhat in the same capacity. Assuming the same conditions as were used in developing Equation 2,

$$M_{hb} = \frac{wd^2 G\gamma_2}{\left(1 - \frac{d}{L}\right)} \qquad (27)$$

Since

$$M_h = M_{ha} + M_{hb}$$

Then,

$$M_h = \gamma_2\left[\frac{wd^2}{1 - \frac{d}{L}}\, G + \frac{A_s dE}{\sqrt{2}}\right] \qquad (28)$$

from which γ_2 may be obtained.

The rotation β_2 due to bending of a Type 2 connection is determined directly from Equation 17. Similarly, the equation for rotation ϕ_r is identical with Equation 18. Thus,

$$\theta_2 = \gamma_2 + \beta_2 + \phi_r$$

as determined from expressions 17, 18 and 28. For a connection of this type joining 8B13 rolled sections (test connection A),

$$\theta_2 = (2.50 + 4.00 + 1.45) \times 10^{-6} M_h \text{ rad.}$$
$$\theta_2 = 7.95 \times 10^{-6} M_h \text{ rad.}$$

II. Type 8B Connections (Vertical and Diagonal Stiffeners). For the Type 8B connections with both vertical and diagonal stiffeners there appears to be less basis for an assumption regarding the transmission of flange forces, F_t, by the diagonal stiffeners.

It will be assumed, instead, that the diagonal acts as if it increased the web area and was distributed uniformly over it. From Equation 2,

$$\gamma_{8B} = \frac{\tau}{G} = \frac{1}{G}\frac{M_h}{d}\frac{\left(1 - \frac{d}{L}\right)}{A_{w'}} \qquad (29)$$

where

$A_{w'}$ = the effective area of the web, $A_{w'} = A_w + A_s'$.

A_s' = equivalent stiffener area.

$$A_s' = \frac{\sqrt{2}db_s t_s}{d} = \sqrt{2}b_s t_s$$

b_s = total width of stiffener.

t_s = stiffener thickness.

The bending rotation, β_{8B}, and rolled-section rotations, ϕ_r, are computed from equations 17 and 18. Thus,

$$\theta_{8B} = (\gamma_{8B} + \beta_{8B} + \phi_r)$$

For connection L tested in the experimental program using an 8B13 section, from equations 17, 18 and 29,

$$\theta_{8B} = (2.51 + 4.00 + 1.45) \times 10^{-6} M_h \text{ rad.}$$
$$\theta_{8B} = 7.96 \times 10^{-6} M_h \text{ rad.}$$

This relationship is plotted in Fig. 22, Part I, as a dot-dash line.

It will be observed that this value is the same as that determined for the Type 2 connection. Although computed on the basis of different assumptions, the calculation of rotation due to shear gave practically identical results.

(*d*) *"Equivalent Length" Rotation Analysis*

In Section II, Part I, "Requirements for Connections," it was mentioned that on the basis of minimum requirements the knee should be as stiff as an equivalent length of the rolled sections joined. Several "equivalent lengths" are shown in Fig. 7 (see Part I).

As is evident from the previous derivations, the calculation of elastic deformations by the simplest methods involves many assumptions. Another point to consider is that such calculations probably are not part of a routine office procedure. Further, calculations of deformation and moment distribution are based on the implied assumption that the knee is "rigid" at the point of intersection of neutral lines but that the rest of the knee behaves as if it were part of the beam or column (Fig. 54, Part I). Thus, a calculation of the type now to be described is of importance.

I. Identical Members. It will first be

assumed that the moment is uniform along the knee length to be considered. Referring to Fig. 59a,

$$M_{AD} = M_{AB} = M_h = M_r$$

Then

$$\phi_A = \phi \Delta L$$

where

ϕ = unit rotation, M_r/EI.

Then

$$\phi_A = \frac{M_h\left(1 - \frac{d}{2L}\right)}{EI}(d + 2r) \quad (30)$$

For the 8B13 rolled shape used in the experimental investigation, for an "r" distance of 1 in.,

$$\phi_A = 7.06 \times 10^{-6} M_h \text{ rad.}$$

This relationship is plotted in Fig. 22, Part I.

II. Dissimilar Members ($d_1 \neq d_2$). Following the same procedure as in the previous section and referring to Fig. 66.

$$\phi_A = \beta_A + \phi_r$$

$$\beta_A = \frac{M_{r1}\left(\frac{d_2}{2}\right)}{EI_1} + \frac{M_{r2}\left(\frac{d_1}{2}\right)}{EI_2}$$

$$\beta_A = \frac{M_h}{2E}\left[\frac{d_2\left(1 - \frac{d_2}{2L}\right)}{I_1} + \frac{d_1\left(1 - \frac{d_1}{L2}\right)}{I_2}\right] \quad (31)$$

Evaluating β_A for connection P and adding the value ϕ_r determined from Equation 22,

$$\phi_A = 3.053 \times 10^{-6} M_h \text{ rad.}$$

This elastic relationship is plotted in Fig. 19, Part I.

The deflection relationship in the elastic range will be discussed in the next section as a part of the plastic analysis.

II. PLASTIC ANALYSIS

Yielding due to flexure alone will be discussed in this section. Thus only connections which do not yield due to shear force within the knee web will be considered. Although in the experimental program plastic deformation due to shear force occurred in one knee, it is recommended that means be taken in design to prevent such failure. It will be assumed, then, that the knee area behaves as if it were a part of the beam and column.

The basis of the plastic deformation relationships is the moment angle-change curve, often referred to as the M-ϕ curve. Methods for computing this function in the early plastic region were described by Luxion and Johnston.[6] The importance of the strain-hardening range and methods of computing the M-ϕ curve in this region have also been described and will be treated in a paper to be published in THE WELDING JOURNAL.*

In Fig. 68 the theoretical and experimental M-ϕ relationships are shown, the calculations being extended into the strain-hardening range. In these computations the results of coupon tests have been used, due account being taken for difference in material properties between the web and the flange. The upper yield point has been disregarded. The experimental curve has been obtained from the test of a simply supported beam, loaded at the third points.

By way of summary, the equations for computing some of the critical points on the complete M-ϕ curve are as follows:

1. Initial Yield

$$\left.\begin{aligned} M_1 &= \sigma_{yF} S \\ \phi_1 &= \frac{\sigma_{yF}}{E\frac{d}{2}} \end{aligned}\right\} \quad (32.1)$$

2. Yielding Penetrated to Bottom of Flange Fillet

$$\left.\begin{aligned} M_2 &= {}^2/_3\sigma_{yw} Z_2 + \sigma_{yF}(Z - Z_2) \\ \phi_2 &= \frac{\sigma_{yw}}{Ey_2} \end{aligned}\right\} \quad (32.2)$$

3. Complete Plasticity ("Plastic Hinge")

$$\left.\begin{aligned} M_3 &= \sigma_{yF}(Z - Z_2) + \sigma_{yw} Z_2 = M_p \\ \phi_3 &= \infty \text{(neglecting strain-hardening)} \\ \phi_3 &= \frac{\epsilon_s}{d/2} \text{(considering strain-hardening)} \end{aligned}\right\} \quad (32.3)$$

4. Strain-Hardening Penetrated to Bottom of Flange Fillet

$$\left.\begin{aligned} M_4 &= M_P + \frac{\sigma_4'}{\left(\frac{d}{2} - y_2\right)} \times \left[I - y_2\left(Z - \frac{Z_2}{3}\right)\right] \\ \phi_4 &= \frac{\epsilon_s}{y_2} \end{aligned}\right\} \quad (32.4)$$

5. Strain-Hardening Penetrated to a Depth Corresponding to an Extreme Fiber Stress Equal to $1.3\sigma_y$

$$\left.\begin{aligned} M_5 &= M_P + \frac{\sigma_5'}{\left(\frac{d}{2} - y_5\right)} \times \left[I - y_5\left(Z - \frac{Z_5}{3}\right)\right] \\ \phi_5 &= \frac{\epsilon_s}{y_5} \end{aligned}\right\} \quad (32.5)$$

In the above expressions,

$Z_2 = wy_2^2$

y_2 = distance from neutral axis to bottom of fillet

$\sigma_4' = \epsilon_s\left(\frac{d}{2y_2} - 1\right)C$

$\sigma_5' = 0.30\sigma_y$,

$y_5 = \frac{d}{2\left(1 + \frac{0.30\sigma_y}{C\epsilon_s}\right)}$,

$Z_5 = w(y_5)^2$.

The influence of axial load (neglected entirely in the discussion) is to cause a reduction in the moment-carrying capacity as predicted by the simple plastic theory. This has been described by Baker[20] and also in Progress Report 2.[7] As seen there,

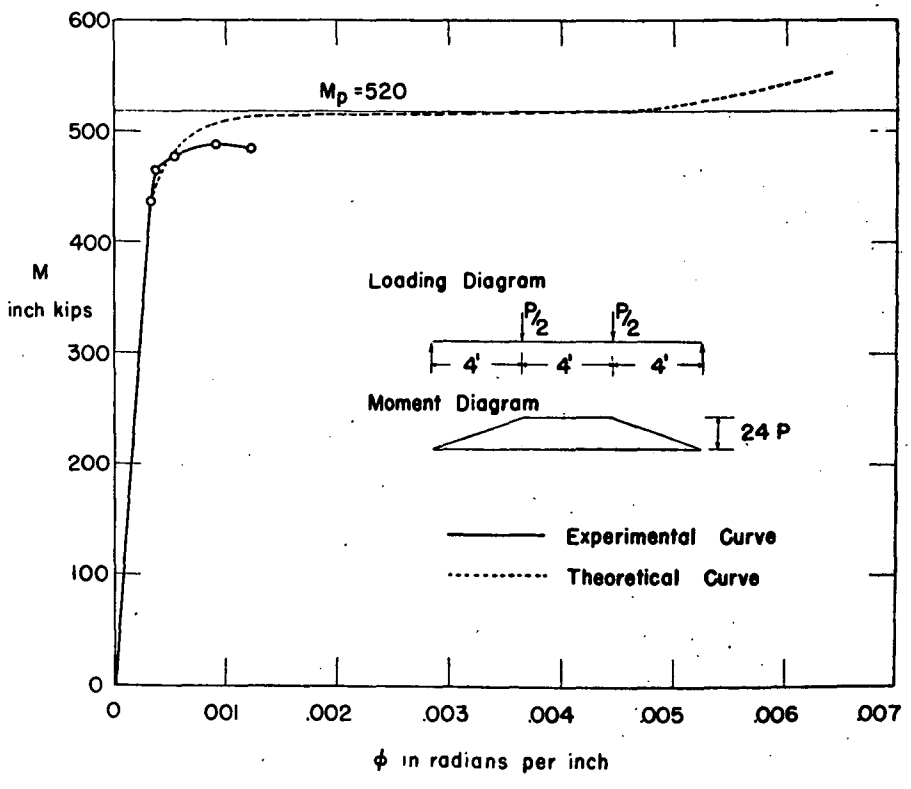

Fig. 68 Moment-curvature relationship (including strain-hardening) for 8B13 beam loaded at the third points

* Paper based on dissertation by C. H. Yang, "The Plastic Behavior of Continuous Beams," Lehigh University, 1951.

axial load does not reduce significantly the ultimate load-carrying capacity until the ratio of axial load to the buckling load exceeds about 0.10. Consequently, its influence will be neglected entirely. Such a ratio is not unusual in frames of the portal type.

1. Rotation

In an earlier part of this report, on the basis of equivalent length of the rolled section, an expression for elastic rotation was developed (Equation 30). This was derived from

$$\phi_A = \phi \Delta L$$

If it is assumed, as implied in the above expression, that the moment is uniform along the equivalent length being considered, then the M-ϕ curve (Fig. 68) in the plastic and strain-hardening ranges may be used. The unit rotations determined from Fig. 68 (Equations 32) are merely multiplied by the equivalent length ΔL. It is only necessary to correct the moment values by the ratio M_h/M_r, since the data of Fig. 68 corresponds to the moment M_r.

The results of this computation have been plotted in Fig. 22, Part I, being indicated by the dotted line. The length over which the rotation was calculated has been assumed equal to the equivalent length of connection L. According to the above assumptions, strain-hardening would not commence until the rotation reached 0.044 radians, a value not within the range of the abscissa.

According to Fig. 62 (a) it is evident that flange stresses decrease toward the outermost end of each stiffener. Thus, so far as the stiffeners are concerned, large deformations would not be expected when the beam reaches the flexural yield point.

If it were assumed that no inelastic rotation occurred within the knee, the M-ϕ_A relationship would be as shown by the dot-dash line in Fig. 69 ($\phi_A = \phi \Delta L = \phi d$). Above M_y and in the region of M_P additional inelastic rotations would merely take place in the rolled section, the M-ϕ_A relationship of which is given by the dotted

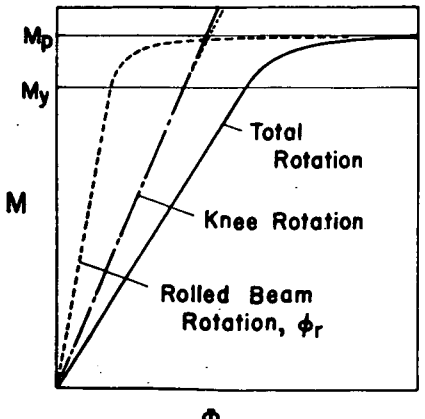

Fig. 69 Moment-curvature relationship based on equivalent length

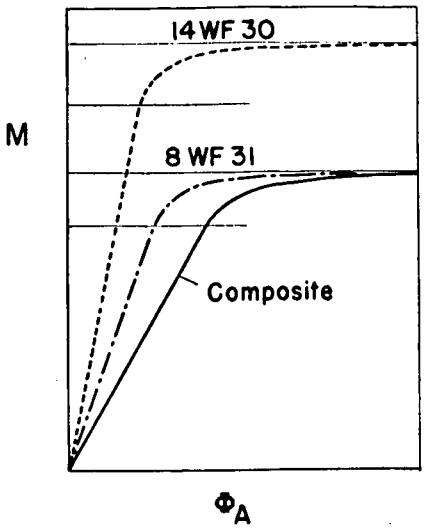

Fig. 70 Moment-curvature relationship (equivalent length) for connection with dissimilar members

curve ($\phi_A = \phi_r = \phi \times 2r$). Thus the M-ϕ_A curve of the complete connection is given by a summation of abscissas to give the solid curve.

The results of such a computation are also plotted in Fig. 22, Part I, as a dashed line.

The same summation of incremental ϕ-values could be used in case the two members were dissimilar. By this method an M-ϕ_A curve could be obtained as shown diagrammatically in Fig. 70. Using the dimensions of test connection P, similar to Fig. 66, ϕ_A for the 14WF30 shape would be computed on the basis that $\Delta L = d_2/2 + r_1$; ΔL for the second member would be $(d_1/2) + r_2$. Since yield occurred in connection P at a low load due to shear force, this flexural calculation will not be carried further in this report.

2. Deflection

A number of methods for computing deflections beyond the elastic limit have been described in the dissertation previously mentioned and are to be the subject of a later paper. Only the simplest of the methods has been used here and the resulting moment-deflection relationship is plotted in Fig. 23, Part I. The curve is computed according to the equations given below. Referring to Fig. 71,

$$\delta = \sqrt{2}\,(\delta_a + \delta_b) \qquad (33)$$

where

δ_a = deflection of the cantilever beam.
δ_b = additional deflection due to rotation of one-half of the knee computed about the intersection of the neutral lines of the members.
δ = deflection along the line of load P.

From Fig. 72,

$$\delta_a = y_1 + y_2 + y_3 \qquad (34)$$

where

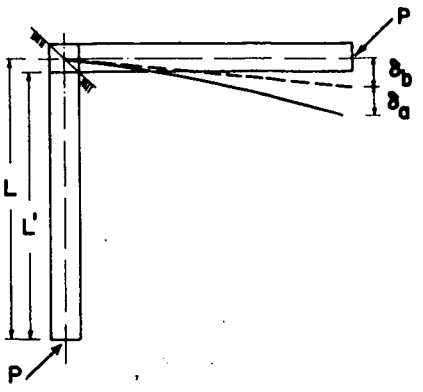

Fig. 71 Connection loading and deflection curve

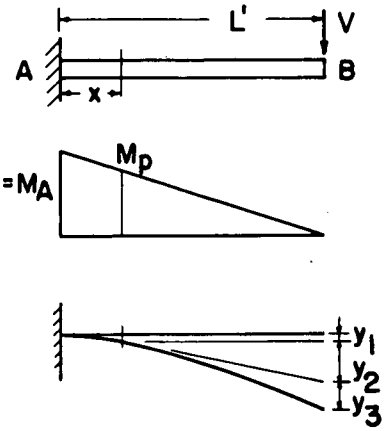

Fig. 72 Cantilever beam deflection

$$\left.\begin{aligned} y_1 &= \frac{1}{CI}\left[\frac{1}{2}M_r x^2 - \frac{M_r x^3}{3L} - \frac{BZx^2}{2}\right] \\ y_2 &= \theta_x (L' - x) \\ y_3 &= \frac{M_A}{3L'EI}(L' - x)^3 \end{aligned}\right\} (34.1)$$

In the above expressions,

$$M_r = M_h\left(1 - \frac{d}{2L}\right)$$

$$x = L'\left(1 - \frac{M_P}{M_r}\right)$$

θ_x = slope at x (Fig. 72)

$$\theta_x = \frac{1}{2CIM_r}\left[M_r^2 - M_P^2 - 2BZ(M_r - M_P)\right] \qquad (34.2)$$

$$L' = L - \frac{d}{2}$$

The value δ_b is given from

$$\delta_b = \frac{1}{2}\phi_A \times L \qquad (35)$$

where ϕ_A is the rotation in the knee and is determined from the modified M-ϕ curve of Fig. 73 which is the basis for this particular method. The "equivalent length" concept is used. For $0 < M_r < M_P$

$$\phi_A = \frac{M_r d}{2EI} \qquad (35.1)$$

and for $M_P < M_r < 1.3M_p$,

$$\phi_A = \left[\frac{M_r - BZ}{CI}\right]\frac{d}{2} \qquad (35.2)$$

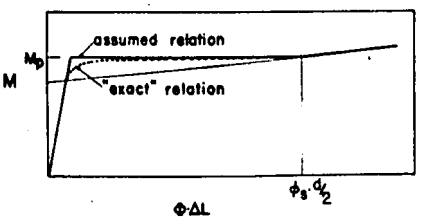

Fig. 73 Assumed and "exact" moment-curvature relationship

As is characteristic of this method for computing the load-deflection relationship the discrepancy between theory and experimental results is the greatest in the early plastic region. This lack of agreement is probably accentuated in these tests by shear deformation, a portion of which is inelastic.

NOTE: The "Discussion of Test Results" and "Summary" is to be included in Part III of this report to appear in a later issue of THE WELDING JOURNAL.

NOMENCLATURE

A = Area of cross section; A_w denotes web area, and A_s the diagonal stiffener area.

B = Intercept on the stress axis of the strain-hardening modulus line extended.

b = flange width.

C = strain-hardening modulus, $d\sigma/d\epsilon$.

d = section depth.

E = Young's modulus.

F = flange force.

f = shape factor, M_p/M_y.

G = modulus of elasticity in shear.

I = moment of inertia.

L = length of connection leg measured from load point to knee center.

L_u = length corresponding to Ld/bt = 600.

ΔL = equivalent length of connection.

M_h = moment at intersection of neutral lines of girder and column, termed "haunch" moment. Subscripts τ and σ denote moments at which yielding occurs due to shear force and flexure, respectively.

M_p = full plastic moment, often termed the "plastic hinge" moment.

M_r = connection moment at junction of rolled beam and knee.

M_y = moment at which the flexural yield-point stress is reached.

N = normal force.

Q = static moment of cross section from outer fiber to neutral axis.

r = distance from end of knee to point of rotation measurement.

S = section modulus, I/c.

t = flange thickness.

V = vertical shear force.

w = web thickness.

Z = plastic modulus; the static moment of the entire cross section about its neutral axis.

β = rotation in connection due to bending.

γ = rotation in connection due to shear.

δ = deflection.

ϵ = unit strain; subscript s denotes unit strain when strain-hardening commences.

θ = rotation.

σ = bending stress; σ_y = lower yield-point stress; subscripts F and W refer to flange and web; subscripts c and t denote compression and tension.

τ = shear stress.

ϕ = rotation per unit length.

ϕ_A = rotation determined on the basis of equivalent length.

ϕ_r = rotation (bending) in rolled section adjacent to knee.

Room Temperature Tensile Tests as an Index of Transition Temperature of Steel Plates

Discussion by W. J. Harris, Jr., J. A. Rinebolt and Richard Raring

Tör, Stout and Johnston have made an interesting analysis of the linear relationship between reduction of area in a tensile test and transition temperature measured by various notch bend and impact tests. However, in view of scatter it is necessary to question whether or not such a relationship can be applied to the prediction of transition temperature as suggested by the authors.

It has recently been shown[1] for pearlitic steels of identical composition and heat treatment that 95% of the transition temperatures (average energy definiton) determined with approximately 300 Charpy V-notch specimens fall in a band 26.8° F. wide. From reduction of area measurements, it should be possible to predict transition temperature within approximately 27° of 95% of the time, if the relationship is to be useful.

A number of data exist which can be analyzed for scatter. Figure 1, which is Fig. 6 of the paper by Tör, Stout and Johnston, shows the scatter band drawn in the original figure as well as a band drawn for purposes of this discussion to include 95% of the points. At constant reduction of area this latter band has a width of 115° F.

Since Tör, Stout and Johnston based their work on two steels in which properties were varied by deformation and subsequent heat treatment it is interesting to compare their conclusions with results of a study[2] in which transition temperature and reduction of area were varied by changes in steel composition at essentially constant microstructure. This study was made on approximately 85 steels in which 13 alloying elements were added one at a time, in increasing amounts to a base analysis. Figure 2 shows the relationship between transition temperature based on the average energy definition and reduction of area of bars pulled at room temperature, and Fig. 3 shows transition temperature based on the 15 ft.-lb. definition plotted in the same manner. The bands containing 95% of the points are approximately 185° F. wide at constant reduction

W. J. Harris, Jr., J. A. Rinebolt and Richard Raring are connected with the Ferrous Alloys Branch, Metallurgy Div., Naval Research Lab., Washington, D. C.

Paper on this subject by **S. S. Tör, R. D. Stout and B. G. Johnston** was published in the September 1950 issue of the *Welding Research Supplement*.